DESIGN OF A GENERIC ROTOR NOISE SOURCE FOR HELICOPTER FUSELAGE SCATTERING TESTS

Jianping Yin[*], jianping.yin@dlr.de; Alex Zanotti[§], zanotti@aero.polimi.it; Karl-Stéphane Rossignol[*], karl-Stephane.Rossignol@dlr.de; Giuseppe Gibertini[§], giuseppe.gibertini@polimi.it; Luigi Vigevano[§], luigi.vigevano@polimi.it

[*]DLR – Germany' [§]Politecnico di Milano - Italy

Abstract

This paper deals with the activities conducted in the GARTEUR Action Group HC/AG-24 to address noise scattering of helicopter rotors in presence of the fuselage. The focus of the paper is on the design for a generic "tail rotor" noise source used in the fuselage scattering study. The main design criterion is that the generic rotor noise source should resemble the main characteristics of the tail rotor with clear harmonic components. A two bladed simplified tail rotor model is considered. The performance of the tail rotor model in terms of thrust and torque with respect to the advance ratio is calibrated in the POLIMI wind tunnel. Acoustic measurements of the tail rotor model were tested in the DLR Acoustic Wind tunnel Braunschweig AWB. The results of the rotor performance and the rotor acoustic characteristics are described. The spectral variations resulting from unsteadiness of the source are explored in both with and without wind. The noise characteristics such as the spectral content, sound levels at fixed distances, and the time varying nature of the sound field are discussed

1. INTRODUCTION

Helicopter noise reduction is a long term objective of research and helicopter industry in view of extending the market to new civil applications, as well as getting prepared to comply with new and increasingly stringent noise regulation. Both the main and the tail rotors (including Fenestron) of a helicopter are major sources of noise and contribute significantly to its ground noise footprint. The research efforts in the past were mainly concentrated on the helicopter rotor noise generation and reduction. Even though the scattering of noise generated by helicopter rotors has been recognized and may have a significant influence on the noise spectra and directivity, there has not been an extensive research effort towards the comprehension of the phenomenon. In order to boost research activities on the noise propagation in presence of the fuselage a specific Action Group (AG24) has been constituted in GARTEUR (the Group for Aeronautical Research and Technology in EURope). The objectives of this AG are (1) to develop and validate numerical prediction methods and (2) to generate a unique noise scattering database through wind tunnel tests using generic configurations [1,2,3,4]. The first wind tunnel activities dealt with acoustic scattering of spheres using monopole sources [3,4]. One purpose of choosing spheres in the test was to verify the accuracy of the complete test system as well as the reliability of the test results. In the second phase of the acoustic scattering tests currently under preparation, the scattering from a generic fuselage, using a realistic tail rotor noise source will be investigated (**Figure 1**). The scattering of tail rotor noise is particularly important because the wavelength of the harmonics is comparable or smaller than the characteristic dimension of the fuselage. This paper will focus on the design activities for a generic "tail rotor" noise source. The main design criterion is that the generic rotor noise source should resemble the main characteristics of the tail rotor, such as an example of a model tail rotor noise spectrum taken from EU Helinovi test (**Figure 2**)[5]. The spectrum demonstrated clear harmonic components of the rotor noise. The design constraint is that the manufacturing cost of the rotor model is small.

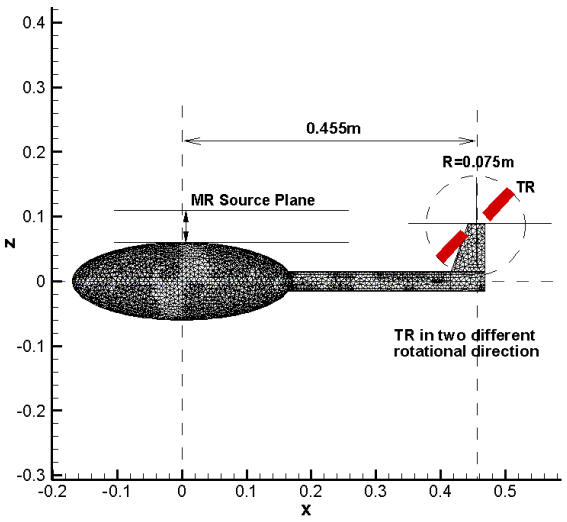

Figure 1: Location of the tail rotor model with respect to the generic fuselage model

Presented at 44th European Rotorcraft Forum, Delft, The Netherlands, 19-20 September, 2018

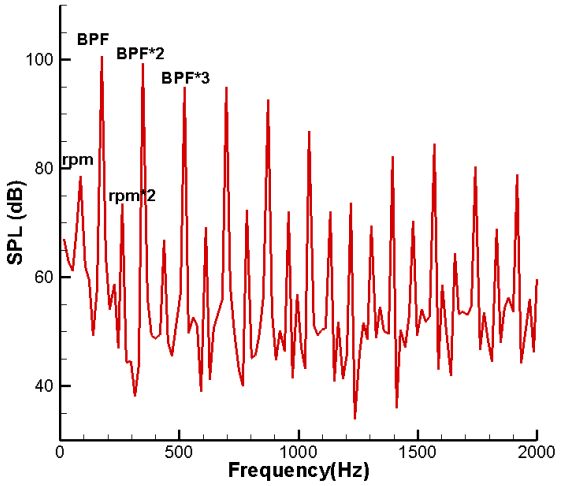

Figure 2: Spectrum at maximum noise position for a two bladed BO105 model tail rotor at 33m/s climb (BPF: Blade Passing Frequency of the tail rotor)

The present paper first illustrates the rotor design, including the criteria on choosing the size, rotational speed, etc., the description of the control system and the aerodynamic calibration results. The test setup for the rotor noise source and the measurement techniques used in the Acoustic Wind tunnel Braunschweig AWB are then described, and an analysis of the noise characteristics of the rotor under different rotational direction as well as wind speed is presented.

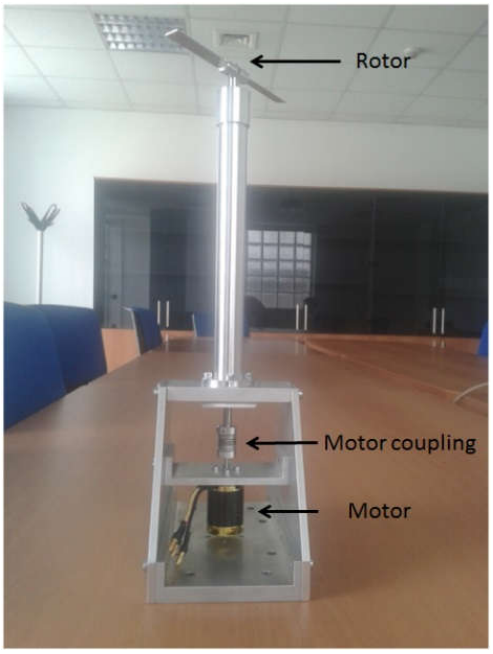

a) Overview of the rotor model

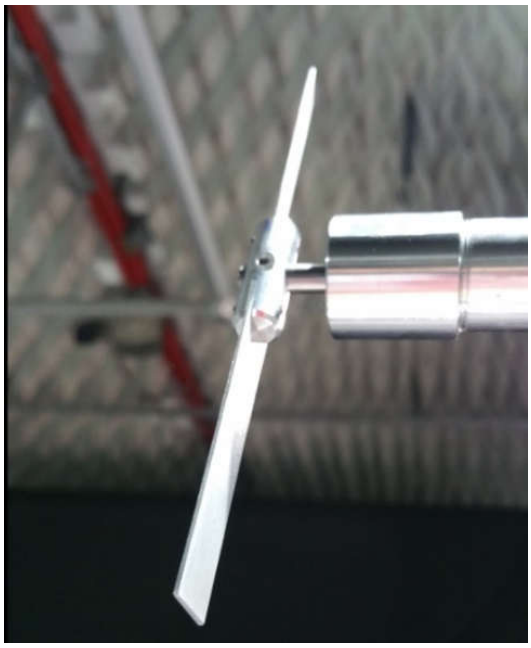

b) zoom of the rotor

Figure 3: The tail rotor model

2. WIND TUNNEL ROTOR MODEL

A simplified two bladed tail rotor model was purposely designed for this test activity, in order to represent a “tail rotor” noise source. It requires proper scaling in terms of tip Mach number and the rotor harmonic frequencies. The rotor has a 0.075 m radius (R) and consists of flat plates blades with 10 mm chord and no twist. The radius dimension has been dictated by the scale of the generic helicopter fuselage with which the tail rotor has to be employed. The blades are mounted to the hub with a fixed pitch angle of 10°, as shown in **Figure 3**. Pitch setting can be reversed so that the rotor can operate either as a tractor or pusher propeller. The rotor is driven by a brush-less low-voltage electrical motor with an electronic controller.

The rotor shaft is coupled by means of a torsional stiff coupling to the motor shaft. A Hall-effect sensor produces one signal per revolution to measure the number of revolutions per minute and to have a reference signal for the synchronization of the measurements. The maximum rotational speed is 23400 RPM, which correspond to a maximum tip Mach number of 0.54 and to a first blade passing frequency (BPF) of 780Hz. After the preliminary test activity aimed at the characterization of the tail rotor source, a fuselage model will be used for the scattering test that resembles a 12.5 times down-scaled BO105

Presented at 44th European Rotorcraft Forum, Delft, The Netherlands, 19-20 September, 2018

fuselage. The main parameters of the tail rotor are reported in **Table 1**.

Property	TR
n° of blades	2
rotor type	hingeless
radius	0.075 m
radius scale factor	12.5
chord	0.01m
root cut-out	0.015 m
solidity	0.085
precone	0°
pretwist	0°/R
pitch-flap coupling	0°
tip Mach number (ISA)	0.54
shaft tilt forward	0°
shaft tilt upward	0°
airfoil	Rectangular flat plate (0.001m thickness)

Table 1: Main parameters of the tail rotor

3. AERODYNAMIC CALIBRATION

Preliminary calibration tests were carried out to evaluate the performance of the isolated tail rotor model in terms of thrust and torque with respect to the advance ratio.

3.1. Calibration set up

The calibration tests were performed in a low-speed closed-return wind tunnel at the Aerodynamics Laboratory of the Department of Aerospace Science and Technology of Politecnico di Milano (POLIMI). The wind tunnel has a rectangular test section with a height of 1.5 m and a width of 1 m. The maximum wind velocity is 55 m/s and the free-stream turbulence level is less than 0.1%. The thrust and torque were measured by means of a strain gauge balance mounted on a supporting strut outside the test section. The frame containing the motor has to be shielded in order to avoid its effect in the balance measurements. The best way was to keep it outside the test section as shown in the set up in **Figure 4**. In this configuration the rotor distance from the floor corresponds to 3R assuring a very small ground effect (less than 1%).

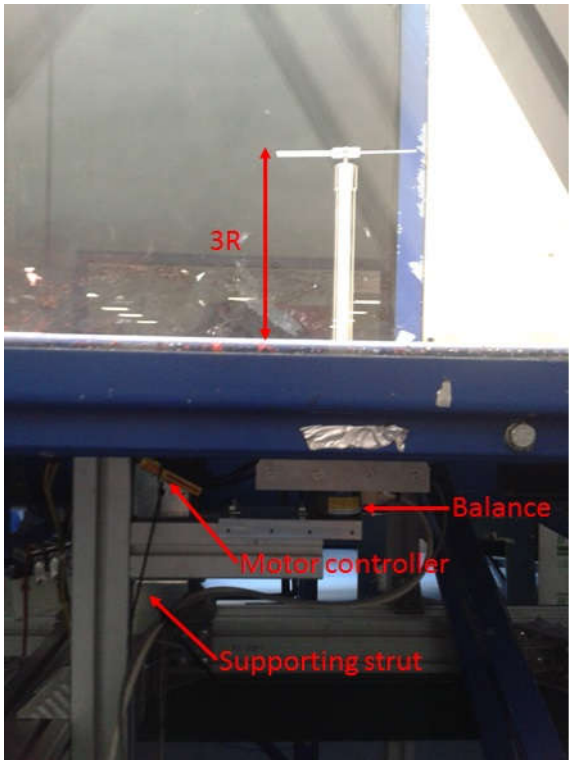

Figure 4: The rotor model set up in the POLIMI wind tunnel

3.2. Calibration results

The wind tunnel tests were carried out with the rotor rotational speed set at 21800 RPM and 23400 RPM. Although the acoustic tests at DLR wind tunnel are planned to be carried out at 21800 RPM due to the higher stability of the rotor at this rotational speed, the calibration tests were performed out at two different rotational speed in order to allow the evaluation of the thrust at slightly different RPM by means of linear interpolation. The loads measurements were performed in hovering and with the wind tunnel free-stream velocity set to 10, 20 and 30 m/s. Moreover, both sense of rotation of the blades were considered during the tests to evaluate the behaviour of the rotor when producing an upward or a downward thrust. The balance and Hall effect sensor signals were acquired over 5 s with a sampling rate of 50 kHz. The tests results are plotted in **Figure 5** and **Figure 6** in terms of absolute thrust and torque coefficients versus the advance ratio. The error bar on the measurement points was evaluated as the standard deviation of the coefficients measured over six repetitions of the tests carried out at 21800 RPM in hovering and with freestream velocity of 30 m/s.

Presented at 44th European Rotorcraft Forum, Delft, The Netherlands, 19-20 September, 2018

The apparent asymmetrical behaviour, i.e. the differences of the thrust in the two opposite rotational directions, is clearly due to the interference of the thick cylindrical pylon.

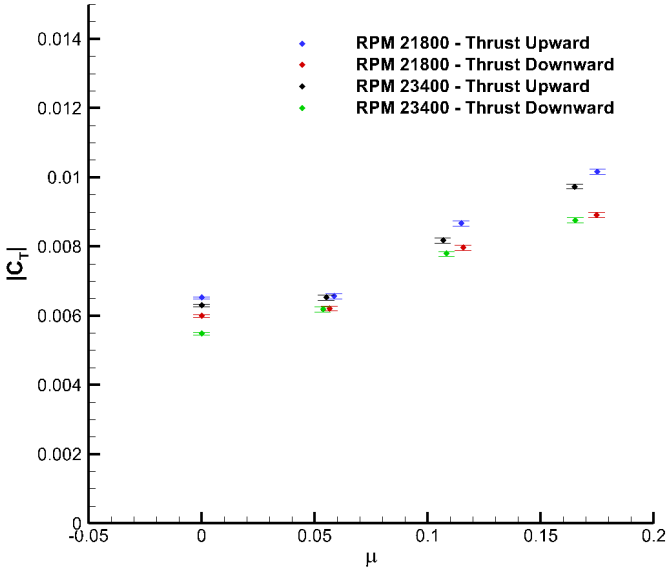

Figure 5: Measured thrust coefficient vs. advance ratio

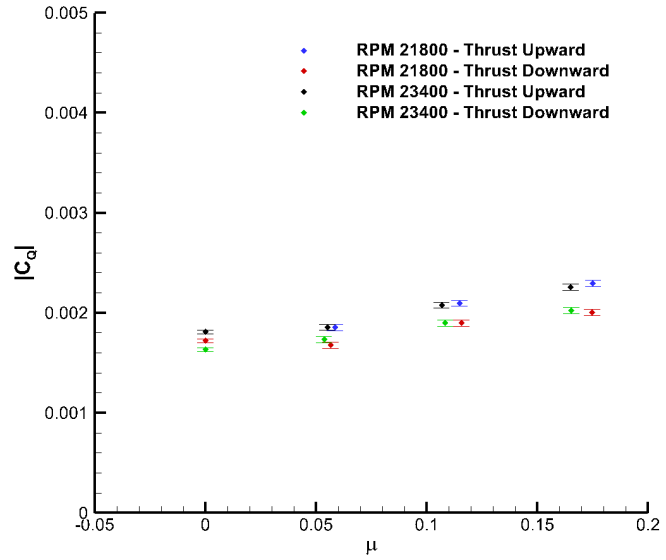

Figure 6: Measured torque coefficient vs. advance ratio

4. ACOUSTIC TEST FOR THE ISOLATED TAIL ROTOR MODEL

4.1. Acoustics Test Setup

Acoustic measurements of the isolated tail rotor model were conducted in the Acoustic Wind tunnel Braunschweig (AWB). The AWB is an open-section anechoic facility with dimensions 1.2 m X 0.8 m, capable of producing a low turbulence stream with maximum velocity up to 65 m/s [6]. The experimental set up with the rotor is shown in **Figure 7**, indicating one of two rotational directions and the corresponding direction of the thrust. A spiral tripping wire on the rotor shaft is used to avoid noise generated by Karman vortex behind the shaft.

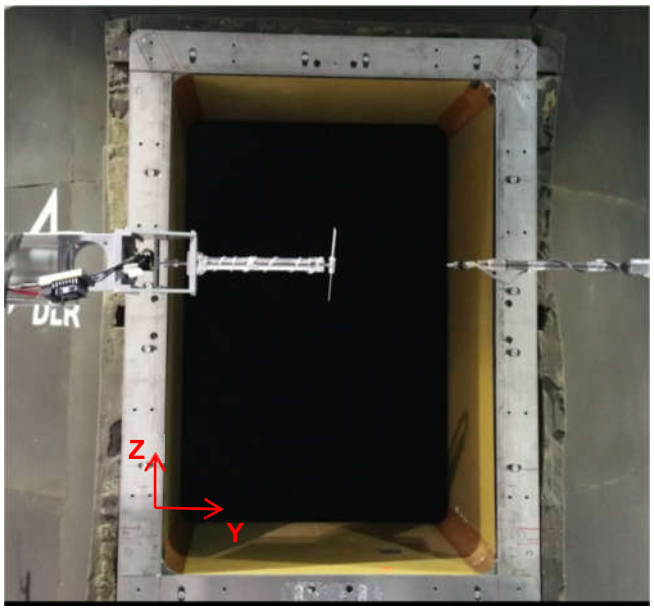

(a)Looking downstream

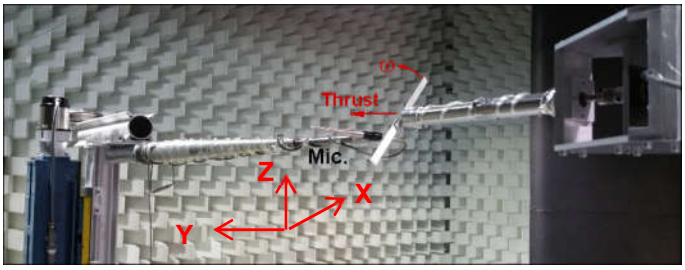

(b) Looking downstream

Figure 7: Rotor noise test set-up in AWB

4.2. Acoustic Instrumentation

A set of microphone positions, as shown in **Figure 8a**, was used to evaluate the noise characteristics as a function of rotational directions of the rotor blades and the wind speed. The microphones on the blue frame represent the one in the rotor rotational-plane. For the case without the wind tunnel flow, the microphone positions represented as the circles in **Figure 8a** are located on 3 arrays numbered with 111,110,109 above the rotor and 3 arrays numbered with 107,106,108 below the rotors. Six microphone positions on each array were measured, which are marked from upstream

Presented at 44th European Rotorcraft Forum, Delft, The Netherlands, 19-20 September, 2018

(000) to downstream (006). **Figure 8b** shows a top view of the microphone arrays. The measurements on each microphone position were done one by one using a microphone fixed on a traverse (see Figure 6). For the case with the wind tunnel flow, the microphone positions represented as the diamonds in **Figure 8a** are located on 3 positions with array number 97.

Measurements are done in-flow using a GRAS 40DP 1/8" inch pressure microphone protected by a nose cap.

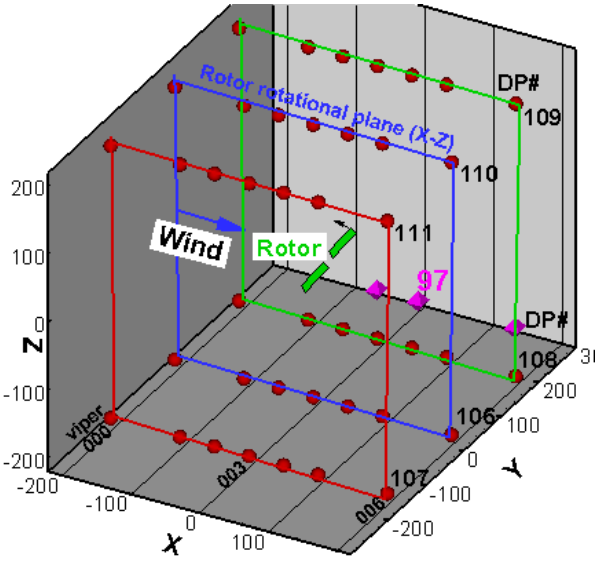

a) all microphone position in 3-D view

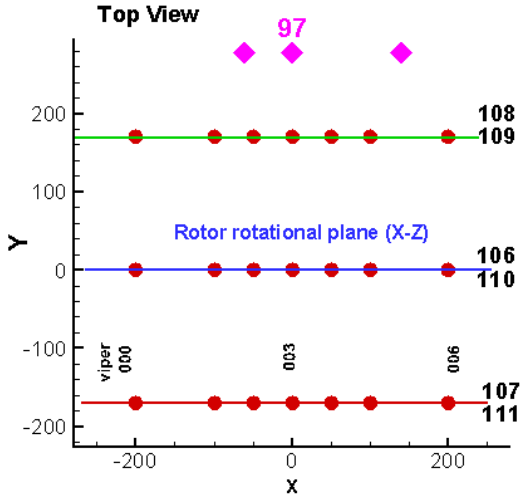

b) all microphone position in top view

Figure 8: Microphone locations

4.3. Data Processing

Data acquisition was done using a sampling rate of 204 kHz. The signals were band-pass filtered between 500 Hz and 110 Hz. For the analysis, a total block length of 16384 samples is considered which provides the necessary frequency resolution for the analysis of the rotor noise tonal components. This implies that each block of data used in the Fourier analysis consists of data acquired over a period corresponding to 29 revolutions of the rotor blades. A 1/revolution trigger signal is acquired in parallel to the acoustic signal to precisely identify the beginning and end of a revolution.

4.4. Acoustic Results

4.4.1. In-plane noise

The frequency behavior varying with time can be checked in the form of a spectrogram. The spectrogram illustrates the multi-tonal, time varying nature of the acoustic signatures of the rotor. The spectrograms taken from microphone 000 and 006 on the array 106 in the rotor rotational plane are given in **Figure 9**. The wind speed for this case is 0m/s. Harmonics of multiple blade passage frequencies (BPFs) are visible as time-varying horizontal traces in the figures. Since the rotor has 2-blades, the blade passage frequencies BPF are 2 times the rotor RPM, which also coincides with the 2nd harmonics of the motor. In addition, harmonics of multiple motor frequencies (RPMs) are also visible in horizontal traces, indicating the presence of noise from the motor system at rpm and its higher harmonics, rpms. Tones are prominent in the spectrograms. The horizontal traces scattering in a narrow band indicate the rotor angular speed is constantly varying, although this time variation is less than 100 rpm, thus less than 0.5% of the nominal rotational speed of the rotor which is 21800 rpm. The operating conditions of the rotor were therefore considered quite stable.

Presented at 44th European Rotorcraft Forum, Delft, The Netherlands, 19-20 September, 2018

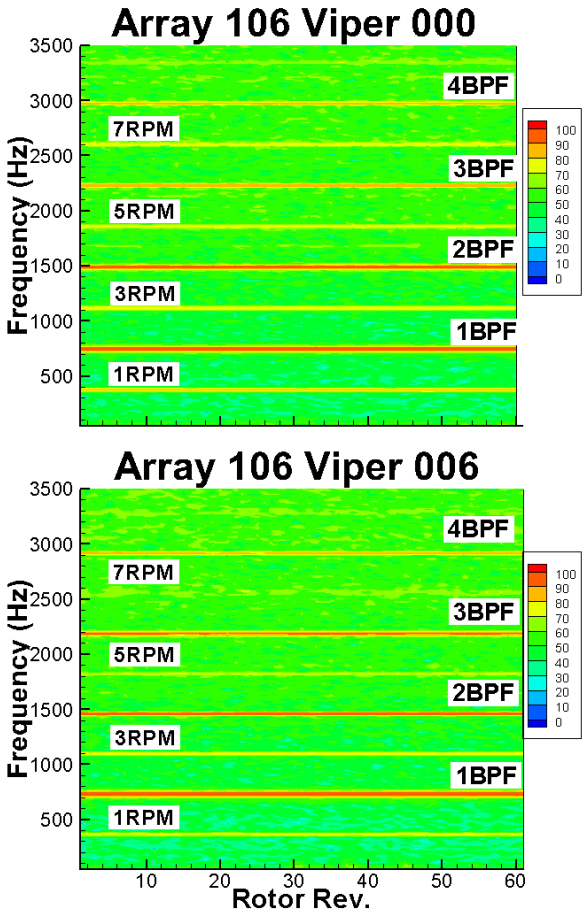

Figure 9: Spectrograms of rotor at V=0m/s

Both the noise spectrum, averaged over complete rotor revolutions and its zoom view are given in **Figure 10** for the no-wind case, again from microphone 000 and 006 on the array 106 in the rotor rotational plane. A combination of rotor, motor and broadband noise is observed. The overall spectrum indicates:

1. the presence of rich rotor harmonics at the BPF and its higher harmonics; the amplitude at blade passage frequencies decays with increasing frequency;
2. the noise from the driving system (motor) at rpm and its higher harmonics;
3. the rotor noise is the dominant source of the noise;
4. with increasing frequency the rotor noise level decays much faster than that of the motor noise, indicating the thickness noise as the dominating source of the rotor generated noise;

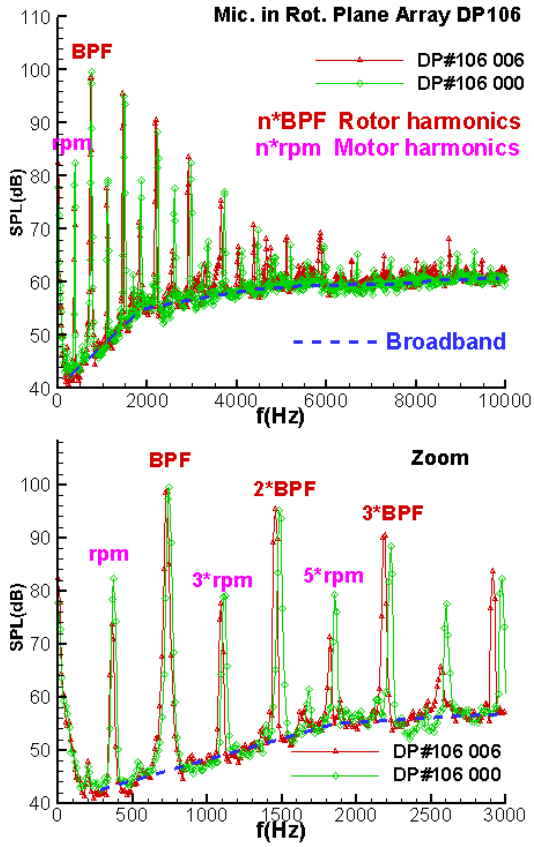

Figure 10: The sound pressure level spectrum taken from microphone 000 and 006 on the array 106 in the rotor rotational plane: top) full frequency range; bottom) zoom view

As the two selected microphones considered in **Figure 9** and **Figure 10** are located in the rotational plane and have the same distance from the rotor hub, the noise spectrum should be the same if the rotor blade was strictly rigid and there was no variation on the rpm and no vibrations. The comparison of the two spectra in **Figure 10** indicates:

1. the difference of the rotor noise level located in rotor harmonics (BPFs) at the two microphones is less than 1dB; the difference was caused by a slight variation of the rpm and the blade deformations as the measurement was done for each microphone separately;
2. there is slight shift in the rotor harmonic frequencies, which is caused by slight variations of the rpm as indicated in the noise spectrogram (**Figure 9**);
3. the amplitude variation of the motor noise between the two microphones is relatively higher than that of the rotor noise;

Presented at 44th European Rotorcraft Forum, Delft, The Netherlands, 19-20 September, 2018

4. Broadband noise (marked as a blue dashed line) can be identified especially in the high frequencies as the consequence of the flat blade profile.

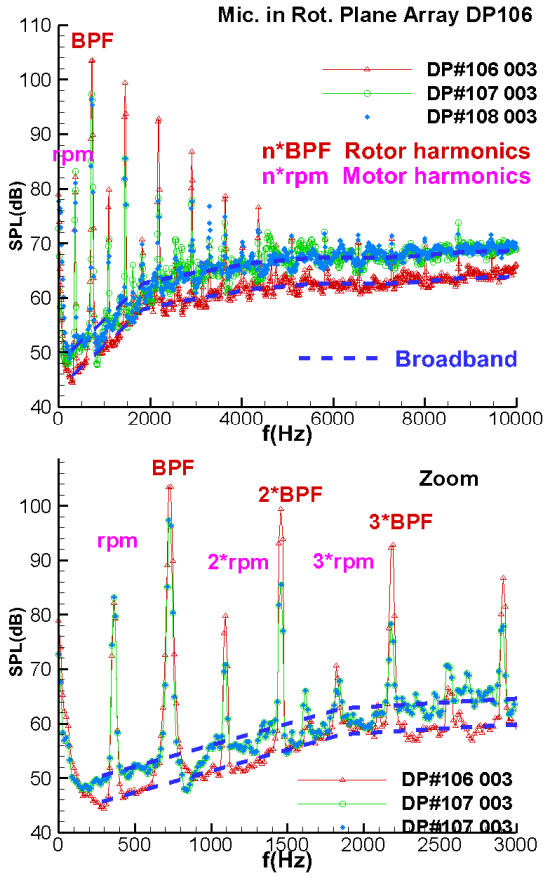

Figure 11: The sound pressure level spectrum taken from microphone 003 on the array 106, 107 and 108: top) full frequency range; bottom) zoom view

4.4.2. Out-of-plane noise

Figure 11 shows the sound pressure level spectrum taken from the microphones located in the middle of the arrays 106, 107 and 108. The higher BPF level for the first 5 rotor harmonics for the microphone in the rotor rotational plane (array 106) demonstrates that the dominant contribution of the in-plane thickness noise decreases with increasing distance from the rotational plane. In addition, an increment of the broadband noise is observed when the microphone is located in a plane away from the rotational plane.

4.4.3. Effect of thrust direction

The rotor can be rotated in two different rotational directions. One of two rotational directions and the corresponding direction of the thrust are given in **Figure 7b**. As the blade has a fixed pitch angle, the reverse of the rotational direction will also change the direction of the thrust.

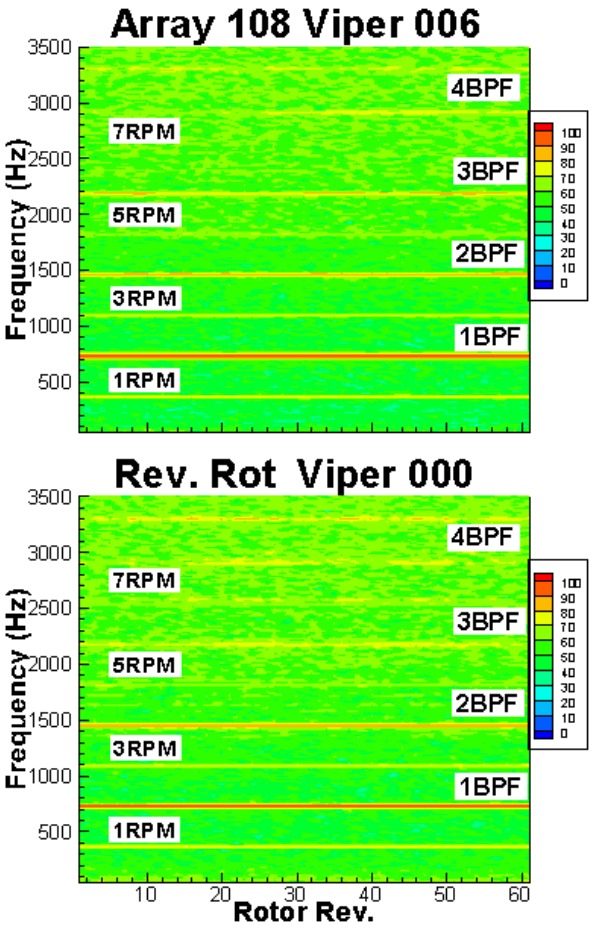

Figure 12: Spectrograms of rotor at V=0m/s

Figure 12 shows the spectrograms taken from two microphones out of rotational plane for the two different rotational directions. The first microphone is located on the array 108 viper 006 and the other on array 107 viper 000 as indicated in **Figure 8**. These two microphones are therefore both located in the thrust side of the rotor and are symmetric relative to the rotor blade tip Mach number and thrust orientation. Therefore both microphones should receive the same acoustic signal, if the deformation of the blade, variation of the rotor rpm and installation effect (rotor support) are all negligible. The first two BPF harmonics are visible for the two rotational directions with quite similar level, while the third BPF is relative weaker in the counter rotating direction (**Figure 12** bottom). The motor harmonics are only clearly visible for the first two harmonics.

Presented at 44th European Rotorcraft Forum, Delft, The Netherlands, 19-20 September, 2018

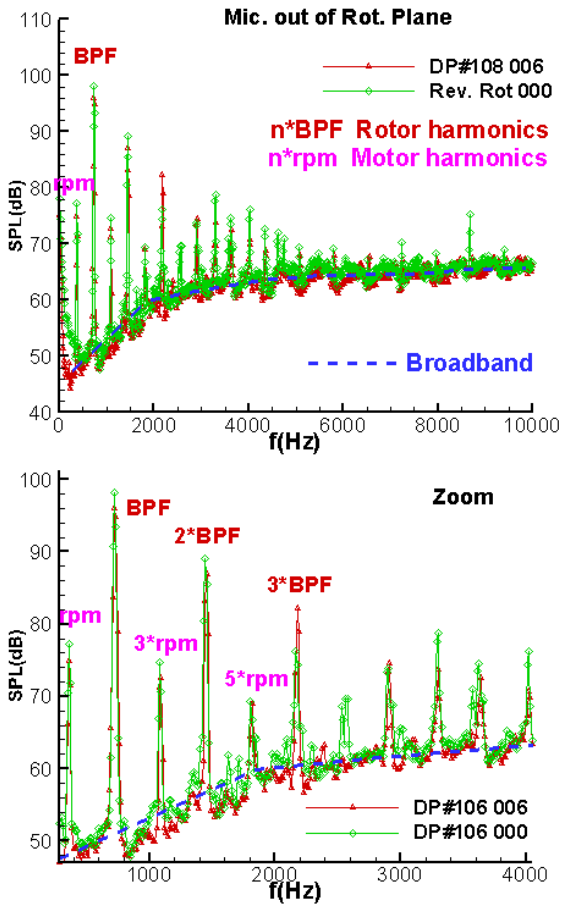

Figure 13: The sound pressure level spectrum for two rotational directions, top) full frequency range; bottom) zoom view

Both the noise spectrum, averaged over a complete rotor revolution and its zoom view for the two rotational directions are given in **Figure 13**. When compared with the spectrum for the microphone located in the rotational plane, shown in **Figure 8**, the amplitude for the higher harmonic BPF tones drops more quickly. This reduction of the noise level indicates, as already pointed out, the reduction of the thickness noise at the out of plane microphones. In addition, the time variation of the rotor rotational speed is smaller, as also indicated in horizontal traces in the **Figure 12**.

The overall spectrum indicates that:

1. the rotor noise is the dominant source of the noise for the first three harmonics;
2. the motor noise is of equal importance than the rotor noise above 3BPF;
3. the broadband noise (marked as blue dashed line) is visible at the high frequencies.

4.4.4. Effect of the mean flow

The effect of the mean flow on the spectrograms is shown in **Figure 14**. The microphone signal is taken from the array 97, as indicated in **Figure 8**, which is further away from the rotor rotational plane.

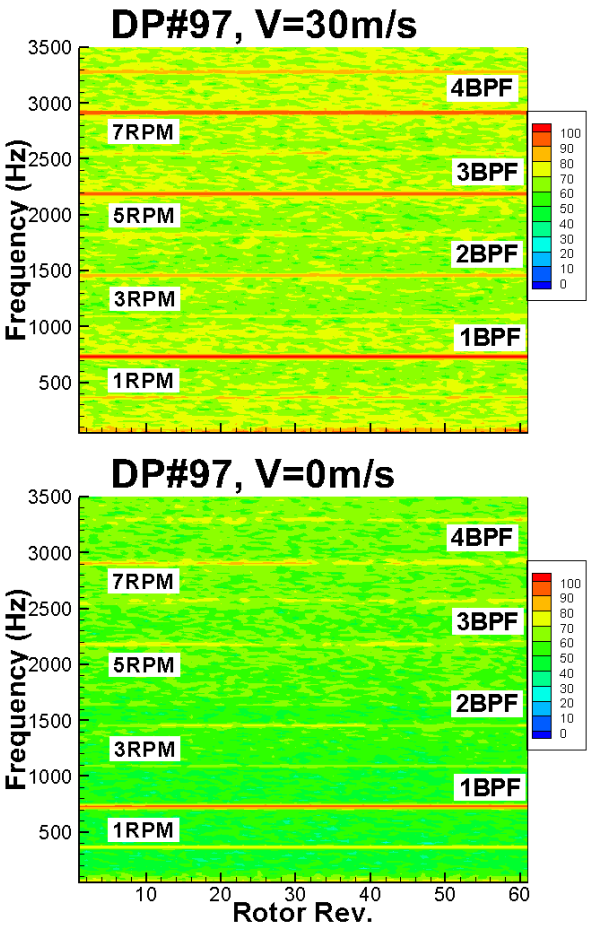

Figure 14: Spectrograms of rotor at V=0, 30m/s

The spectrogram at V=0m/s (**Figure 14**, bottom) shows further reduction on thickness noise as the microphone is located further away from the rotor rotational plane. Only the first rotor BPF as well as the first motor harmonic is continually visible throughout the measurement time, marked by horizontal traces in the figures. The effect of the flow clearly increases the aerodynamic loading noise for the high BPFs, as shown in **Figure 14** top. This behavior can be seen more in detail in the comparison of the averaged spectrum as shown in **Figure 15**. The increase of the loading noise at high BPF harmonics as well as broadband noise can be clearly observed at V=30m/s.

Presented at 44th European Rotorcraft Forum, Delft, The Netherlands, 19-20 September, 2018

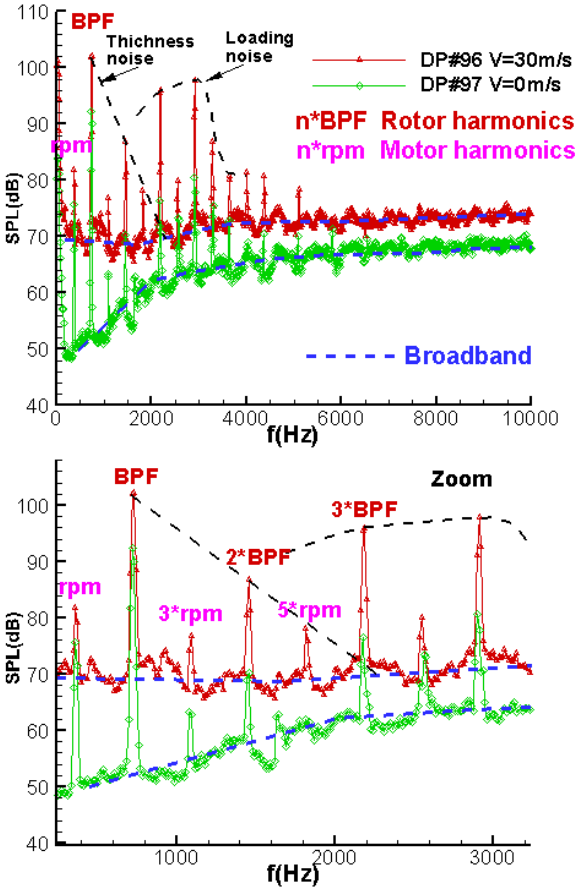

Figure 15: The sound pressure level spectrum for two wind speed, top) full frequency range; bottom) zoom view

5. CONCLUDING REMARKS

In this paper, the design activities for a generic "tail rotor" noise source and the experimental investigations on the characteristics of the tail rotor in terms of the aerodynamic and acoustic are presented. The following concluding remarks can be drawn:

- The spectrograms shows that the rotor speed is constantly varying, but the conditions for the rotor were quite stable since this variation is within 0.5% of the nominal rotational speed;
- The tail rotor noise is a combination of rotor, motor and broadband noise;
- The characteristics of the rotor noise indicate clear harmonic components, especially in the case with flow: therefore the main design requirement is fulfilled;
- Rotor harmonic noise is the dominant source of noise;
- In the case without flow, thickness noise is dominant; it represents the main noise contribution in the rotor rotational plane, while its amplitude reduces fairly quickly when moving away from the rotational plane;
- When the tail rotor operates in a fluid flow, the aerodynamic loading noise is increased at BPF harmonics higher than the second;
- The rotor model will be used as tail rotor noise source in the noise scattering from the fuselage in the next GARTEUR AG24 test campaign.

6. REFERENCES

[1] J. Yin, M. Barbarino, H. Brouwer, G. Reboul, M. Gennaretti, G. Bernardini, C. Testa, L. Vigevano, "Helicopter Fuselage Scattering Effects for Exterior/Interior Noise Reduction", Terms of Reference for the GARTEUR Action Group HC/AG-24, April 2015.

[2] D. Bianco, M. Barbarino, J. Yin, M. Lummer, G. Reboul, M. Gennaretti, G. Bernardini, C. Testa, "Acoustical methods towards accurate prediction of rotorcraft fuselage scattering", 42nd European Rotorcraft Forum, September 5-8, Lille, France, Paper 62, 2016

[3] J. Yin, K.-S. Rossignol, J. Bulté, "Acoustic scattering experiments on spheres for studying helicopter noise scattering", 42nd European Rotorcraft Forum, September 5-8, Lille, France, Paper 127, 2016

[4] J. Yin, K.-S. Rossignol, M. Barbarino, D. Bianco, C. Testa, H. Brouwer, S. Janssen, G. Reboul, L. Vigevano, G. Bernardini, M. Gennaretti, J. Serafini, C. Poggi, "Acoustical Methods and Experiments for Studying Rotorcraft Fuselage Scattering". 43rd European Rotorcraft Forum (ERF) 2017, 12-15 September 2017, Milan.

[5] J. Yin, B.G. van der Wall and S. Oerlemans, "Acoustic wind tunnel tests on helicopter tail rotor noise (HeliNOVI)", Journal of the American Helicopter Society, Vol. 53, No. 3, 2008, pp. 226-239.

[6] M. Pott-Pollenske and J. Delfs, "Enhanced Capabilities of the Aeroacoustic Wind Tunnel Braunschweig." 14th AIAA/CEAS Aeroacoustics Conference, No. 2008-2910, May 2008

Copyright Statement

Presented at 44th European Rotorcraft Forum, Delft, The Netherlands, 19-20 September, 2018

party material included in this paper, to publish it as part of their paper. The authors confirm that they give permission, or have obtained permission from the copyright holder of this paper, for the publication and distribution of this paper as part of the ERF proceedings or as individual offprints from the proceedings and for inclusion in a freely accessible web-based repository.

Presented at 44th European Rotorcraft Forum, Delft, The Netherlands, 19-20 September, 2018